


Article

Synthesis and Crystal Structure of the Zintl Phases $\text{Na}_2\text{CaCdSb}_2$, $\text{Na}_2\text{SrCdSb}_2$ and $\text{Na}_2\text{EuCdSb}_2$

Bayram Saparov^{1,2} and Svilen Bobev^{1,*} ¹ Department of Chemistry and Biochemistry, University of Delaware, Newark, DE 19716, USA² Department of Chemistry and Biochemistry, University of Oklahoma, Norman, OK 73019, USA

* Correspondence: bobev@udel.edu

Abstract: This work details the synthesis and the crystal structures of the quaternary Zintl phases $\text{Na}_2\text{CaCdSb}_2$, $\text{Na}_2\text{SrCdSb}_2$ and $\text{Na}_2\text{EuCdSb}_2$. They are isostructural and their noncentrosymmetric structure is with the space group $Pmc2_1$ (Pearson code $oP12$). All structural work is carried out via single-crystal X-ray diffraction methods. The structure features $[\text{CdSb}_2]^{4-}$ layers of corner-shared CdSb_4 tetrahedra, which are stacked along the b -crystallographic axis and are separated by cations. The results from the structure refinements suggest that in addition to full cation ordering, which is typical for this structure, there also exists a possibility for an accommodation of a small degree of cation disorder.

Keywords: antimonides; crystal structure; thermoelectrics; Zintl phases



Citation: Saparov, B.; Bobev, S. Synthesis and Crystal Structure of the Zintl Phases $\text{Na}_2\text{CaCdSb}_2$, $\text{Na}_2\text{SrCdSb}_2$ and $\text{Na}_2\text{EuCdSb}_2$. *Inorganics* **2022**, *10*, 265. <https://doi.org/10.3390/inorganics10120265>

Academic Editors: Marco Fronzi, Paolo Mele and Giovanna Latronico

Received: 26 October 2022

Accepted: 14 December 2022

Published: 18 December 2022

Publisher's Note: MDPI stays neutral with regard to jurisdictional claims in published maps and institutional affiliations.



Copyright: © 2022 by the authors. Licensee MDPI, Basel, Switzerland. This article is an open access article distributed under the terms and conditions of the Creative Commons Attribution (CC BY) license (<https://creativecommons.org/licenses/by/4.0/>).

1. Introduction

Since the discovery of Yb_2CdSb_2 and Ca_2CdSb_2 [1], which adopt different structures with similar motifs— Yb_2CdSb_2 crystallizes in the noncentrosymmetric space group $Cmc2_1$, whereas Ca_2CdSb_2 crystallizes in the centrosymmetric space group $Pnma$ —our group has been conducting systematic studies on related quaternary compounds [2–8]. First, we investigated the solid solutions $A_xM_{2-x}\text{CdSb}_2$, where A and M stand for the alkaline-earth metals Ca, Sr and Ba, and the nominally divalent rare-earth metals Eu and Yb [2]. The structures of all currently found $A_xM_{2-x}\text{CdSb}_2$ phases are isotypic with the Yb_2CdSb_2 structure, featuring $[\text{CdSb}_2]^{4-}$ layers of corner-shared CdSb_4 tetrahedra. The layers are stacked along the b -crystallographic axis and are separated by cations (Figure 1). The placement of the different cations in all cases point at site preferences governed by simple spatial requirements—the larger cations prefer the crystallographic position with octahedral coordination of Sb atoms, which is referred to as the “interlayer” site. The smaller cations prefer to occupy the more compact site with square pyramidal arrangement of Sb atoms surrounding it, which is referred to as the “intra-layer” site. For a more comprehensive treatment of the cation site preferences from a computational perspective, the reader is directed to the paper dealing with those problems in the related phosphides $\text{Ba}_x\text{Sr}_{2-x}\text{CdP}_2$ [7,8]. Of note is the fact that the “2-1-2” structure in question has become synonymous with low thermal conductivity, which is an important facet in modern thermoelectrics development. As a result, other research teams have utilized the flexibility of the structure to design new materials for thermoelectric energy conversion [9–12] and second harmonic generation [13].

Extensions of the above work in a slightly different direction were the experiments directed at heterovalent substitutions of the divalent metal cations in Yb_2CdSb_2 and Ca_2CdSb_2 . To date, we have succeeded in the synthesis and the accurate structural characterization of the Zintl compounds $\text{K}_2\text{SrCdSb}_2$, $\text{K}_2\text{BaCdSb}_2$ and $\text{Na}_2\text{YbCdSb}_2$ [2]. These quaternary phases crystallize with a novel type, with a noncentrosymmetric orthorhombic structure akin to that of Yb_2CdSb_2 , where the mono- and divalent cations are ordered and occupy distinct crystallographic sites. The experimental data for $\text{Na}_2\text{CaCdSb}_2$, $\text{Na}_2\text{SrCdSb}_2$ and

$\text{Na}_2\text{EuCdSb}_2$ at that time were insufficient to unequivocally establish the crystal structure, and only the unit-cell parameters were available for the latter.

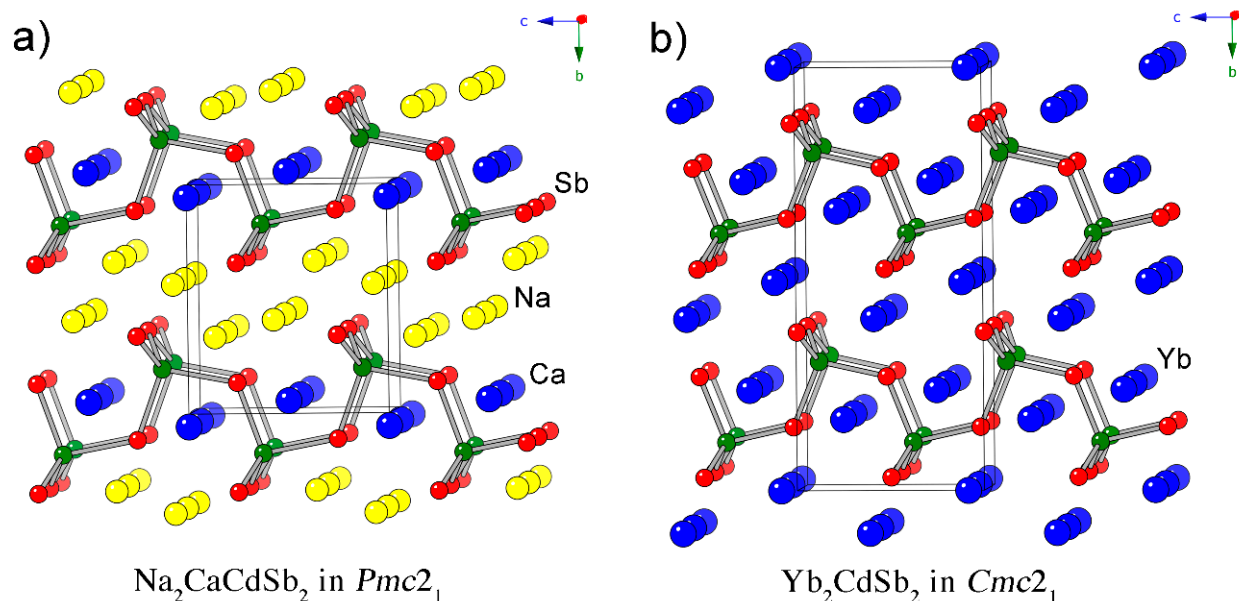


Figure 1. Side-by-side comparison between the crystal structure of $\text{Na}_2\text{CaCdSb}_2$ (a) and that of Yb_2CdSb_2 (b). Both projections are along the a -crystallographic axis. Bonds are drawn only between Cd (green) and Sb (red) atoms, emphasizing the polyanionic $[\text{CdSb}_2]^{4-}$ layers. Unit cells are outlined.

With this paper, we report the structures of these three compounds, established from single-crystal X-ray diffraction methods. The new results suggest that, in addition to full cation ordering, the structure is also able to accommodate some cation disorder.

2. Results

Details of the data collection and selected crystallographic parameters are summarized in Tables 1 and 2. For brevity, throughout the text, the simplified chemical formulae $\text{Na}_2\text{CaCdSb}_2$, $\text{Na}_2\text{SrCdSb}_2$ and $\text{Na}_2\text{EuCdSb}_2$ will be used instead of the refined formulae.

As discussed previously, the structure is very much alike to that of Yb_2CdSb_2 , which is also noncentrosymmetric and crystallizes orthorhombically [1]. The latter has the space group $Cmc2_1$ (Pearson symbol $oC20$), while the structure under consideration herein has the space group $Pmc2_1$ (Pearson symbol $oP12$). In both, there are $[\text{CdSb}_2]^{4-}$ layers made of corner-shared CdSb_4 tetrahedra, which are stacked along the b -crystallographic axis. In both structures, the polyanionic layers are separated by slabs of cations. The main difference is that there are two divalent cations per formula unit in the $Cmc2_1$ structure, while in the $Pmc2_1$ one, there are three—two monovalent sodium cations formally substitute one alkaline-earth or rare-earth. The additional cation positions in $\text{Na}_2\text{CaCdSb}_2$, $\text{Na}_2\text{SrCdSb}_2$ and $\text{Na}_2\text{EuCdSb}_2$ necessitate the removal of the base-centering and halving the unit-cell volume. This is the most distinguishable difference between these two structures, which are schematically represented side-by-side in Figure 1.

There are six unique crystallographic positions in the asymmetric unit (Table 3), including two sodium, one calcium (or strontium or europium), one cadmium and two antimony sites, all in special positions with site symmetries m . All refined anisotropic displacement parameters are normal, despite the observed disorder (a figure showing a structural representation with anisotropic displacement parameters is provided as Supplementary Material). Na1 exhibits a somewhat enlarged atomic displacement parameter compared to Na2, but this must be an artifact of the greater coordination number (CN), since U_{eq} for Na2 is larger than U_{eq} for Na1 in all refined structures (Table 3). Another noteworthy crystallographic feature is the uneven variation of the unit-cell vectors a , b and c as a function of the size of

the alkaline-earth metal. This is not unexpected, considering the fact that the magnitude of the *a*- and *c*-lattice parameters should correlate most strongly with the size of Ca, Sr and Eu, while the *b*-lattice parameter will be in correlation with the cation disorder, which is not uniform across the series.

Table 1. Selected single-crystal data collection and structure refinement parameters for Na₂CaCdSb₂ and Na₂SrCdSb₂.

Empirical Formula	Na _{1.95} (4)Ca _{1.05} CdSb ₂	Na _{1.99} (1)Sr _{1.01} CdSb ₂
Formula weight	442.81	490.15
Temperature (K)	170 (2)	170 (2)
Radiation, λ	Mo K α , 0.71073 Å	Mo K α , 0.71073 Å
Space group, <i>Z</i>	<i>Pmc</i> 2 ₁ , 2	<i>Pmc</i> 2 ₁ , 2
<i>a</i> (Å)	4.6720 (11)	4.7724 (10)
<i>b</i> (Å)	9.083 (2)	9.0514 (19)
<i>c</i> (Å)	7.8201 (19)	8.0470 (17)
<i>V</i> (Å ³)	331.86 (14)	347.61 (13)
ρ_{cal} (g/cm ³)	4.43	4.68
μ (cm ⁻¹)	120.5	184.0
Goodness-of-fit on <i>F</i> ²	1.114	1.020
Unique reflections	933	980
Refined parameters	42	40
<i>R</i> ₁ (<i>I</i> > 2 σ _{<i>I</i>}) ^a	0.0263	0.0224
<i>wR</i> ₂ (<i>I</i> > 2 σ _{<i>I</i>}) ^a	0.0675	0.0409
<i>R</i> ₁ (all data) ^a	0.0267	0.0240
<i>wR</i> ₂ (all data) ^a	0.0678	0.0414
Largest diff. peak and hole (e ⁻ /Å ³)	1.99 and -1.10	1.01 and -0.83
CCDC deposition no.	2215539	2215541

^a $R_1 = \sum ||F_o| - |F_c|| / \sum |F_o|$; $wR_2 = [\sum [w(F_o^2 - F_c^2)^2] / \sum [w(F_o^2)^2]]^{1/2}$, where $w = 1 / [\sigma^2 F_o^2 + (AP)^2 + (BP)]$ and $P = (F_o^2 + 2F_c^2) / 3$. *A* and *B* are the respective weight coefficients (see the CIFs).

Table 2. Selected single-crystal data collection and structure refinement parameters for two independent samples of Na₂EuCdSb₂.

Empirical Formula	Na _{2.07} (1)Eu _{0.93} CdSb ₂	Na ₂ EuCdSb ₂
Formula weight	544.81	553.84
Temperature (K)	170 (2)	170 (2)
Radiation, λ	Mo K α , 0.71073 Å	Mo K α , 0.71073 Å
Space group, <i>Z</i>	<i>Pmc</i> 2 ₁ , 2	<i>Pmc</i> 2 ₁ , 2
<i>a</i> (Å)	4.7478 (14)	4.7441 (11)
<i>b</i> (Å)	9.001 (3)	9.099 (2)
<i>c</i> (Å)	7.977 (2)	7.9766 (18)
<i>V</i> (Å ³)	340.90 (17)	344.34 (13)
ρ_{cal} (g/cm ³)	5.31	5.34
μ (cm ⁻¹)	193.5	197.8
Goodness-of-fit on <i>F</i> ²	1.091	1.070
Unique reflections	953	969
Refined parameters	40	38
<i>R</i> ₁ (<i>I</i> > 2 σ _{<i>I</i>}) ^a	0.0314	0.0168
<i>wR</i> ₂ (<i>I</i> > 2 σ _{<i>I</i>}) ^a	0.0778	0.0394
<i>R</i> ₁ (all data) ^a	0.0323	0.0170
<i>wR</i> ₂ (all data) ^a	0.0784	0.0395
Largest diff. peak and hole (e ⁻ /Å ³)	3.85 and -1.02	1.36 and -1.39
CCDC deposition no.	2215538	2215540

^a $R_1 = \sum ||F_o| - |F_c|| / \sum |F_o|$; $wR_2 = [\sum [w(F_o^2 - F_c^2)^2] / \sum [w(F_o^2)^2]]^{1/2}$, where $w = 1 / [\sigma^2 F_o^2 + (AP)^2 + (BP)]$ and $P = (F_o^2 + 2F_c^2) / 3$. *A* and *B* are the respective weight coefficients (see the CIFs).

Table 3. Atomic coordinates of the atoms and their equivalent isotropic displacement parameters U_{eq} ^a for Na₂CaCdSb₂, Na₂SrCdSb₂ and Na₂EuCdSb₂.

Atom	Site	<i>x</i>	<i>y</i>	<i>z</i>	U_{eq} (Å ²)
Na ₂ CaCdSb ₂					
Ca ^b	2 <i>a</i>	0	0.0569 (2)	0.0000 (3)	0.014 (1)
Na1	2 <i>b</i>	1/2	0.4204 (5)	0.0501 (5)	0.025 (1)
Na2 ^c	2 <i>a</i>	0	0.3298 (4)	0.3699 (5)	0.019 (1)
Sb1	2 <i>b</i>	1/2	0.1199 (1)	0.2849 (1)	0.013 (1)
Sb2	2 <i>a</i>	0	0.6577 (1)	0.2667 (1)	0.015 (1)
Cd	2 <i>b</i>	1/2	0.1868 (1)	0.6601 (1)	0.016 (1)
Na ₂ SrCdSb ₂					
Sr ^b	2 <i>a</i>	0	0.0571 (1)	0.0000 (1)	0.015 (1)
Na1	2 <i>b</i>	1/2	0.4224 (4)	0.0406 (6)	0.027 (1)
Na2 ^c	2 <i>a</i>	0	0.3325 (3)	0.3652 (4)	0.018 (1)
Sb1	2 <i>b</i>	1/2	0.1260 (1)	0.2856 (1)	0.014 (1)
Sb2	2 <i>a</i>	0	0.6563 (1)	0.2500 (1)	0.016 (1)
Cd	2 <i>b</i>	1/2	0.1863 (1)	0.6571 (1)	0.018 (1)
Na ₂ EuCdSb ₂					
Eu ^b	2 <i>a</i>	0	0.0558 (1)	0.0000 (1)	0.015 (1)
Na1	2 <i>b</i>	1/2	0.4244 (7)	0.0398 (9)	0.032 (1)
Na2 ^c	2 <i>a</i>	0	0.3307 (4)	0.3635 (5)	0.023 (1)
Sb1	2 <i>b</i>	1/2	0.1265 (1)	0.2857 (1)	0.017 (1)
Sb2	2 <i>a</i>	0	0.6564 (1)	0.2522 (1)	0.020 (1)
Cd	2 <i>b</i>	1/2	0.1847 (1)	0.6588 (1)	0.020 (1)

^a U_{eq} is defined as one third of the trace of the orthogonalized U_{ij} tensor. ^b Refined occupancies: for Ca/Na = 0.90 (3)/0.10; for Sr/Na = 0.937 (5)/0.063; and for Eu/Na = 0.813 (5)/0.187. ^c Refined occupancies: for Na2/Ca = 0.83 (5)/0.17; for Na2/Sr = 0.921 (6)/0.079; and for Na2/Eu = 0.904 (5)/0.096.

As discussed already, the simplest way to relate the structure to that of the parent Yb₂CdSb₂ is to consider the aliovalent substitution of the interlayer Yb²⁺ cations by twice as many Na⁺ cations in way that the overall electron count is preserved. Using Na₂CaCdSb₂ and Yb₂CdSb₂ as examples, the following formulae breakdowns can be suggested: (Na⁺)₂(Ca²⁺)(Cd²⁺)(Sb³⁻)₂ and (Yb²⁺)₂(Cd²⁺)(Sb³⁻)₂.

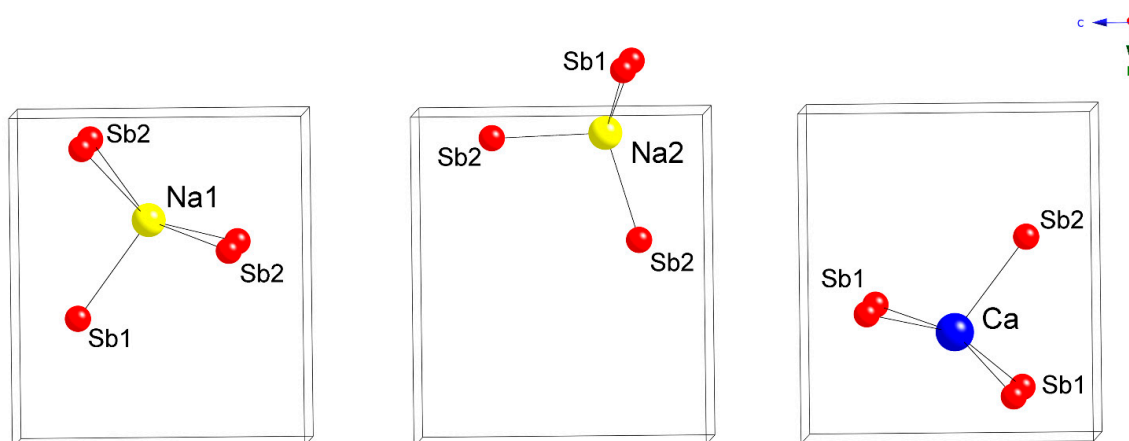
Since the [CdSb₂]⁴⁻ layers made of corner-shared CdSb₄ tetrahedra are the same in both structures, it is obvious that packing of the interlayer Yb²⁺ cations in Yb₂CdSb₂ will have to differ from that of the Na⁺ cations in Na₂CaCdSb₂. Indeed, in Yb₂CdSb₂, the interlayer Yb atoms have CN6 (distorted octahedral), while in Na₂CaCdSb₂, Na1 has CN5 (distorted square-pyramidal) and Na2 has CN4 (distorted tetrahedral). Relevant distances from all four refined structures are tabulated in Tables 4 and 5. The coordination environments of the three cationic sites in Na₂CaCdSb₂ are depicted in Figure 2. Careful inspection of the data shows that Na2 in particular is very tightly coordinated by the neighboring Sb atoms with Na2–Sb distances approaching the sum of the single-bonded radii of Sb (Pauling radius 1.39 Å) and Na (Pauling radius 1.57 Å) [14]. For the two known structures with K, namely, K₂SrCdSb₂ and K₂BaCdSb₂, the respective K2–Sb distances are on the order of 3.4 Å [2], also matching the sum of the single-bonded radii of Sb and K (Pauling radius 2.02 Å) [14]. This finding is unusual, since the electronic structure calculations for K₂SrCdSb₂ and K₂BaCdSb₂ indicate the mostly “passive” (i.e., space-filler and electron-donor) role of the alkali metals in these compounds, with minimal contribution from K near the Fermi level [2]. By comparison, the Sr and Ba atoms make more significant contributions to the DOS in the same energy window. This has also been the case for some other ternary antimonides such as Ba₃Cd₂Sb₄ [15], Ba₂Cd₂Sb₃ [16] and Ba₂ZnSb₂ [17], which we have studied as well.

Table 4. Selected interatomic distances (Å) in Na₂CaCdSb₂ and Na₂SrCdSb₂.

Atom Pair	Distance (Å)	Atom Pair	Distance (Å)
Na ₂ CaCdSb ₂		Na ₂ SrCdSb ₂	
Cd–Sb2 (×2)	2.8543 (7)	Cd–Sb2 (×2)	2.8777 (7)
Cd–Sb1	2.952 (1)	Cd–Sb1	3.011 (1)
Cd–Sb1	2.997 (1)	Cd–Sb1	3.039 (1)
Sb1–Cd	2.952 (1)	Sb1–Cd	3.011 (1)
Sb1–Cd	2.997 (1)	Sb1–Cd	3.039 (1)
Sb2–Cd (×2)	2.8543 (7)	Sb2–Cd (×2)	2.8777 (7)
Ca–Sb2	3.170 (2)	Sr–Sb2	3.289 (1)
Ca–Sb1 (×2)	3.278 (2)	Sr–Sb1 (×2)	3.3712 (9)
Ca–Sb1 (×2)	3.296 (2)	Sr–Sb1 (×2)	3.3790 (9)
Ca–Cd (×2)	3.453 (2)	Sr–Cd (×2)	3.485 (1)
Na1–Sb2 (×2)	3.297 (3)	Na1–Sb2 (×2)	3.416 (3)
Na1–Sb1	3.290 (4)	Na1–Sb1	3.329 (4)
Na1–Sb2 (×2)	3.601 (3)	Na1–Sb2 (×2)	3.608 (3)
Na2–Sb2	3.086(4)	Na2–Sb2	3.074 (3)
Na2–Sb1 (×2)	3.087 (2)	Na2–Sb1 (×2)	3.098 (2)
Na2–Sb2	3.105 (4)	Na2–Sb2	3.098 (3)

Table 5. Selected interatomic distances (Å) in for two independent samples of Na₂EuCdSb₂.

Atom Pair	Distance (Å)	Atom Pair	Distance (Å)
Na _{2.07} (1)Eu _{0.93} CdSb ₂		Na ₂ EuCdSb ₂	
Cd–Sb2 (×2)	2.870 (1)	Cd–Sb2 (×2)	2.8713 (7)
Cd–Sb1	2.978 (2)	Cd–Sb1	2.993 (1)
Cd–Sb1	3.022 (2)	Cd–Sb1	3.028 (1)
Sb1–Cd	2.978 (2)	Sb1–Cd	2.993 (1)
Sb1–Cd	3.022 (2)	Sb1–Cd	3.028 (1)
Sb2–Cd (×2)	2.870 (1)	Sb2–Cd (×2)	2.8713 (7)
Eu–Sb2	3.259 (2)	Eu–Sb2	3.2510 (8)
Eu–Sb1 (×2)	3.352 (1)	Eu–Sb1 (×2)	3.3484 (7)
Eu–Sb1 (×2)	3.354 (1)	Eu–Sb1 (×2)	3.3485 (6)
Eu–Cd (×2)	3.453 (1)	Eu–Cd (×2)	3.4731 (7)
Na1–Sb2 (×2)	3.380 (5)	Na1–Sb2 (×2)	3.378 (2)
Na1–Sb1	3.322 (7)	Na1–Sb1	3.331 (3)
Na1–Sb2 (×2)	3.587 (5)	Na1–Sb2 (×2)	3.623 (3)
Na2–Sb2	3.063 (4)	Na2–Sb2	3.074 (3)
Na2–Sb1 (×2)	3.066 (3)	Na2–Sb1 (×2)	3.114 (2)
Na2–Sb2	3.103 (4)	Na2–Sb2	3.115 (4)

**Figure 2.** Cation coordination polyhedra in the crystal structure of Na₂CaCdSb₂.

3. Discussion

The observations above imply that, although the title compounds fit the classical description of Zintl phases [18], some degree of covalency of the interactions for the presumed "cations" should also be expected.

In the context of the presented results, it is instructive to draw attention to the fact that, in three of the four refined structures, Na2 is the position that shows "heavier" electron density than Na. In the case of the Ca-bearing compound, the freely refined site occupation factor (SOF) for Na2 was 112%, but in the case of the Eu-bearing compound, the freely refined SOF for Na2 was 156%. At the same time, Na1 had an SOF that did not deviate much from unity and never showed a tendency to be over 100%. The same applies to the Sb and Cd positions as well. The SOF of Ca in $\text{Na}_2\text{CaCdSb}_2$ was 98%, the SOF of Sr in $\text{Na}_2\text{SrCdSb}_2$ was 96% and the SOF of Eu in $\text{Na}_2\text{EuCdSb}_2$ was 84%. There was another $\text{Na}_2\text{EuCdSb}_2$ crystal, from an independent experiment with a different Na:Eu ratio, that showed no SOF deviations (Table 2). Given the above, we proposed a model with a statistical admixture of Na/Ca, Na/Sr and Na/Eu on both Ca (Sr and Eu) and Na2 sites, which was refined successfully (Tables 1 and 2). All final refined compositions are very close to the ideal "2-1-1-2", indicating that the number of available valence electrons is still near the optimal value despite the disorder on both cation sites.

There are other possible structural models that can be proposed to explain the experimental observations described in the previous paragraph. Although the previous electronic structure calculations have suggested little covalency of the K–Sb interactions, one may notice that Na2–Sb and Cd–Sb distances are not too far off (Tables 4 and 5). In our schematic representation of the structure in Figures 1 and 2, only bonds that can be considered as mostly covalent (i.e., Cd–Sb interactions) are drawn. If one takes the liberty to consider the 3.1 Å Na2–Sb bond as covalent, a different schematic representation emerges, as seen in Figure 3. In this view, the structure can now be said to be more 3D, rather than layered, and derived from the well-known TiNiSi structure type (ternary variant of CeCu_2) [19]. From the many compounds adopting that structure, the most useful comparison that can be made is to the structure of NaCdSb [20]. Simply put, in NaCdSb ($= \text{Na}_2\text{Cd}_2\text{Sb}_2$), if 50% of the Cd atoms are replaced by Na atoms, the resultant chemical formula will be Na_3CdSb_2 . Naturally, since the chemical bonding for this arrangement requires 18 electrons per formula unit for TiNiSi: $4(\text{Ti}) + 10(\text{Ni}) + 4(\text{Si}) = 18$; and 8 electrons per formula for NaCdSb : $1(\text{Na}) + 2(\text{Cd}) + 5(\text{Sb}) = 8$, as shown by Nussli et al. [19], the bonding in the derived Na_3CdSb_2 will not be optimized. The dimensionality of the framework must be reduced as a result, and further steps must be taken to satisfy the octets of all atoms.

Considering the structural analogy drawn between $\text{Na}_2\text{CaCdSb}_2$ and NaCdSb , we may propose a different explanation for the observed anomalies concerning the SOF on Na2 site—what if the "heavy" Na2 was a partially occupied Cd, i.e., $\text{NaCaCd}_{2-x}\text{Sb}_2$? Model refinements showed that the SOF of this Cd atom in $\text{NaCaCd}_{2-x}\text{Sb}_2$ was just 26%, while in $\text{NaEuCd}_{2-x}\text{Sb}_2$, where the Na-overoccupancy was extreme, the SOF of the Cd atom refined instead of Na was ca. 36%. This means that such hypothetical structures will be severely deprived of valence electrons to exist as variants of NaCdSb . Therefore, we argue that $\text{NaCaCd}_{2-x}\text{Sb}_2$, $\text{NaSrCd}_{2-x}\text{Sb}_2$ and $\text{NaEuCd}_{2-x}\text{Sb}_2$ are unlikely structural models, even though precedents for similar structures with a large amount of vacancies exist, such as $\text{NaIn}_{0.67}\text{Bi}$ [21], for example.

We also considered models with statistical admixtures of Na/Cd on the Na2 site, as well as statistical admixtures Na/Ca, Na/Sr and Na/Eu on the Ca, Sr and Eu sites. They could be refined satisfactorily and the CIFs are provided as Supplementary Material. Here, we will just give the final refined formulae from these trial refinements: $\text{Na}_{1.96}\text{Ca}_{0.98}\text{Cd}_{1.04}\text{Sb}_2$, $\text{Na}_{2.01}\text{Sr}_{0.94}\text{Cd}_{1.05}\text{Sb}_2$ and $\text{Na}_{2.05}\text{Eu}_{0.81}\text{Cd}_{1.14}\text{Sb}_2$. Distinguishing these refined compositions from the ones in Tables 1 and 2 via independent chemical analyses is clearly impossible. Both structural scenarios are plausible from the chemical bonding point of view, as the electron counts are nearly identical and satisfy the valence rules. The observation that the overoccupancy on the Na2 site was observed to increase

in the order $\text{Ca} > \text{Sr} > \text{Eu}$, i.e., from lighter to heavier, taken together with the fact that we were able to obtain two crystals from two independent samples of $\text{Na}_2\text{EuCdSb}_2$, where the nominal Na: Eu were varied and the resultant structure refinements were in correlation with that (Table 2) appear to support the hypothesis for Na/Ca, Na/Sr and Na/Eu disorder on both sites. However, the model with statistical admixtures of Na/Cd on the Na2 site, and Na/Ca, Na/Sr and Na/Eu on the Ca, Sr and Eu sites, cannot be ruled out completely. This requires additional experimental and computational work, which is beyond the scope of this study.

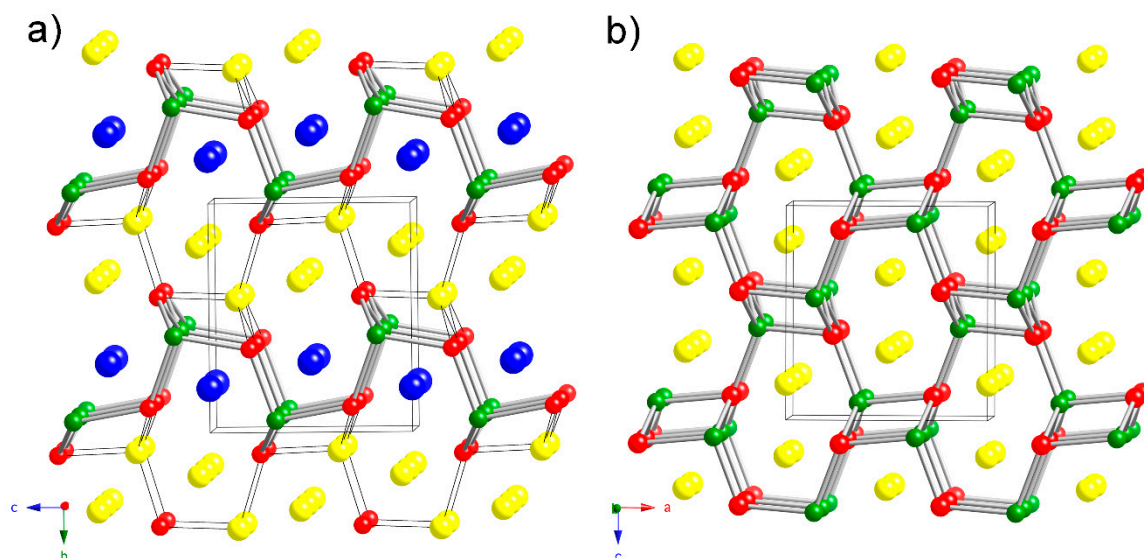


Figure 3. Side-by-side comparison between the crystal structure of $\text{Na}_2\text{CaCdSb}_2$ (a) and that of NaCdSb (TiNiSi-structure type) (b). The judiciously drawn Cd–Sb bonds (cylinders) and the 3.1 Å Na2–Sb bonds (black lines) emphasize the $[\text{NaCdSb}_2]^{3-}$ framework in $\text{Na}_2\text{CaCdSb}_2$ (a) and its similarity to the $[\text{Cd}_2\text{Sb}_2]^{2-}$ framework in NaCdSb (b). Unit cells are outlined and the origin of the unit cell in (a) is shifted in order to facilitate the comparison. Color code: Na in yellow, Ca in blue, Cd in green and Sb in red.

4. Materials and Methods

The synthesis is described in detail in the prior publication focused on the synthesis and the crystal structures of $\text{K}_2\text{SrCdSb}_2$, $\text{K}_2\text{BaCdSb}_2$ and $\text{Na}_2\text{YbCdSb}_2$ [2]. The experimental data for making $\text{Na}_2\text{CaCdSb}_2$, $\text{Na}_2\text{SrCdSb}_2$ and $\text{Na}_2\text{EuCdSb}_2$ are mentioned there as well, and the existence of these compounds with the same crystal structure as $\text{K}_2\text{SrCdSb}_2$, $\text{K}_2\text{BaCdSb}_2$ and $\text{Na}_2\text{YbCdSb}_2$ was inferred from the respective unit-cell parameters. Here, we only reiterate the need to maintain inert atmosphere every step of the way, because most of the complications with the synthesis and the crystallographic studies arise from the extreme air- and moisture-sensitivity, which necessitates due diligence—work in a glove-box filled with argon gas (with oxygen and moisture levels below 1 ppm) or under vacuum with both starting materials and reaction products.

In the earlier study, X-ray powder diffraction data were taken using a Rigaku MiniFlex powder diffractometer, which was operated inside a nitrogen-filled glove box to prevent contact of the samples with air and moisture. For this follow up work, X-ray powder diffraction patterns were not pursued. All the characterization steps were done via single-crystal X-ray diffraction.

The crystals were small and did not have well defined morphologies. Air stability was an issue (vide supra), therefore single crystals were selected in the glove-box (under a microscope) and cut to desired dimensions (around 0.1 mm) with a scalpel. This was easily done because the crystals were very brittle. Two techniques were used to handle the crystals prior to mounting them on the goniometer—either covering them in dry Paratone-N oil and scooping them with MitiGen plastic loops or sealing them in thin-walled glass capillaries.

The intensity data were acquired using a nitrogen gas stream to alleviate the problem with air-sensitivity. Temperature was maintained at 170 K throughout the experiments. Multiple crystals had to be tried before the ones with the best quality were identified. Intensity data were collected using a Bruker SMART CCD diffractometer. The Bruker-supplied software packages [22,23] were used to manage data collection and for the integration of the measured reflections. Absorption correction was applied using SADABS [24]. Refinements by least-square minimizations on F^2 were carried out with the aid of the SHELXL program [25]. The atomic coordinates from the previous reports on related antimonide phases [2] were suitable starting models, and the first refinement cycles quickly yielded reasonable conventional residual factors. However, there were some issues with the displacement parameters, which required checking the site occupation factors (SOFs) of all atomic positions. In three of the four refinements, the site occupied by the divalent metals (Ca, Sr and Eu) were found to be slightly underoccupied, while one of the two Na-sites exhibited unphysical overoccupancy (SOF exceeded 150% in the case of the Eu-compound). Considering the Zintl concept and the drive for attaining optimized bonding in this structure, the metal sites had to be modeled as statistically distributed Ca/Na, Sr/Na and Eu/Na on these two positions. Doing so allowed us to achieve proper fitting and very reasonable agreement between the displacement parameters for all atoms in each structure (Table 3). Final difference Fourier maps, in all cases, were featureless, and the final refined formulae are listed in Tables 1 and 2. Alternative structural models with Cd contributing to the “heavy” Na2 were also considered, as discussed in Section 3. The results from these trial refinements are available as supporting information.

Supplementary Materials: The following supporting information can be downloaded at: <https://www.mdpi.com/article/10.3390/inorganics10120265/s1>, Figure showing a structural representation of $\text{Na}_{1.96}\text{Ca}_{0.98}\text{Cd}_{1.04}\text{Sb}_2$ with anisotropic displacement parameters; CIF from the refinements for $\text{Na}_2\text{EuCdSb}_2$ (cation-ordered) where the Eu and Na2 sites are refined with freed SOFs. CIFs from the refinements for $\text{Na}_{1.96}\text{Ca}_{0.98}\text{Cd}_{1.04}\text{Sb}_2$, $\text{Na}_{2.01}\text{Sr}_{0.94}\text{Cd}_{1.05}\text{Sb}_2$ and $\text{Na}_{2.05}\text{Eu}_{0.81}\text{Cd}_{1.14}\text{Sb}_2$, where disorder was modeled as statistical admixtures of Na/Cd on the Na2 site, and Na/Ca, Na/Sr and Na/Eu admixing on the Ca, Sr and Eu sites.

Author Contributions: Conceptualization, B.S. and S.B.; methodology, formal analysis, B.S. and S.B.; investigation, B.S. and S.B.; resources, S.B.; data curation, S.B.; writing—original draft preparation, S.B.; writing—review and editing, S.B.; supervision, S.B.; project administration, S.B.; funding acquisition, S.B. All authors have read and agreed to the published version of the manuscript.

Funding: This research was funded by the US Department of Energy through a grant DE-SC0008885.

Data Availability Statement: The corresponding crystallographic information files (CIF) for all structures have been deposited with CSD, and the data for this paper can be obtained free of charge via <http://www.ccdc.cam.ac.uk/conts/retrieving.html> (accessed on 13 December 2022) (or from the CCDC, 12 Union Road, Cambridge CB2 1 EZ, UK; Fax: +44-1223-336033; E-mail: deposit@ccdc.cam.ac.uk). Depository numbers are 2215538–2215541.

Conflicts of Interest: The authors declare no conflict of interest.

References

1. Xia, S.-Q.; Bobev, S. Cation-anion interactions as structure directing factors: Structure and bonding of Ca_2CdSb_2 and Yb_2CdSb_2 . *J. Am. Chem. Soc.* **2007**, *129*, 4049–4057. [[CrossRef](#)] [[PubMed](#)]
2. Saporov, B.; Saito, M.; Bobev, S. Syntheses, and crystal and electronic structures of the new Zintl phases $\text{Na}_2\text{ACdSb}_2$ and K_2ACdSb_2 ($A = \text{Ca, Sr, Ba, Eu, Yb}$): Structural relationship with Yb_2CdSb_2 and the solid solutions $\text{Sr}_{2-x}\text{A}_x\text{CdSb}_2$, $\text{Ba}_{2-x}\text{A}_x\text{CdSb}_2$ and $\text{Eu}_{2-x}\text{Yb}_x\text{CdSb}_2$. *J. Solid State Chem.* **2011**, *184*, 432–440. [[CrossRef](#)]
3. Ogunbunmi, M.O.; Baranets, S.; Bobev, S. Structural complexity and tuned thermoelectric properties of a new polymorph of the Zintl phase Ca_2CdSb_2 with a non-centrosymmetric monoclinic structure. *Inorg. Chem.* **2022**, *61*, 10888–10897. [[CrossRef](#)] [[PubMed](#)]
4. Ovchinnikov, A.; Darone, G.; Saporov, B.; Bobev, S. Exploratory work in the quaternary system of Ca–Eu–Cd–Sb: Synthesis, crystal, and electronic structures of new Zintl solid solutions. *Materials* **2018**, *11*, 2146. [[CrossRef](#)]

5. Wang, J.; Yang, M.; Pan, M.-Y.; Xia, S.-Q.; Tao, X.-T.; He, H.; Darone, G.M.; Bobev, S. Synthesis, crystal and electronic structures, and properties, of the new pnictide semiconductors A_2CdPn_2 ($A = Ca, Sr, Ba, Eu; Pn = P, As$). *Inorg. Chem.* **2011**, *50*, 8020–8027. [[CrossRef](#)]
6. Saparov, B.; Broda, M.; Ramanujachary, K.V.; Bobev, S. New quaternary Zintl phases—Synthesis, crystal and electronic structures of $KA_2Cd_2Sb_3$ ($A = Ca, Sr, Ba, Eu, Yb$). *Polyhedron* **2010**, *29*, 456–462. [[CrossRef](#)]
7. Balvanz, A.; Qu, J.; Baranets, S.; Ertekin, E.; Gorai, P.; Bobev, S. New n -type Zintl phases for thermoelectrics: Discovery, structural characterization, and band engineering of the compounds A_2CdP_2 ($A = Sr, Ba, Eu$). *Chem. Mater.* **2020**, *32*, 10697–10707. [[CrossRef](#)]
8. Qu, J.; Balvanz, A.; Baranets, S.; Bobev, S.; Gorai, P. Computational design of thermoelectric alloys through optimization of transport and dupability. *Mater. Horiz.* **2022**, *9*, 720–730. [[CrossRef](#)]
9. Cooley, J.A.; Promkhan, P.; Gangopadhyay, S.; Donadio, D.; Pickett, W.E.; Ortiz, B.R.; Toberer, E.S.; Kauzlarich, S.M. High Seebeck coefficient and unusually low thermal conductivity near ambient temperatures in layered compound $Yb_{2-x}Eu_xCdSb_2$. *Chem. Mater.* **2018**, *30*, 484–493. [[CrossRef](#)]
10. Kim, K.; Lee, J.; Shin, S.; Jo, H.; Moon, D.; Ok, K.M.; You, T.-S. Chemical driving force for phase-transition in the $Ca_{2-x}RE_xCdSb_2$ ($RE = Yb, Eu; 0.11(1) \leq x \leq 1.36(2)$) system. *Cryst. Growth Des.* **2020**, *20*, 746–754. [[CrossRef](#)]
11. Devlin, K.P.; Chen, S.; Donadio, D.; Kauzlarich, S.M. Solid solution $Yb_{2-x}Ca_xCdSb_2$: Structure, thermoelectric properties, and quality factor. *Inorg. Chem.* **2021**, *60*, 13596–13606. [[CrossRef](#)] [[PubMed](#)]
12. Hauble, A.K.; Crawford, C.M.; Adamczyk, J.M.; Wood, M.; Fettingner, J.C.; Toberer, E.S.; Kauzlarich, S.M. Deciphering defects in $Yb_{2-x}Ca_xCdSb_2$ and their impact on thermoelectric properties. *Chem. Mater.* **2022**, *34*, 9228–9239. [[CrossRef](#)]
13. Sun, Y.; Lin, C.; Chen, J.; Xu, F.; Yang, S.; Li, B.; Yang, G.; Luo, M.; Ye, N. α - Ca_2CdP_2 and β - Ca_2CdP_2 : Two polymorphic phosphide-based infrared nonlinear crystals with distorted NLO-active tetrahedral motifs realizing large second harmonic generation effects and suitable band gaps. *Inorg. Chem.* **2021**, *60*, 7553–7560. [[CrossRef](#)] [[PubMed](#)]
14. Pauling, L. *The Nature of the Chemical Bond*, 3rd ed.; Cornell University Press: Ithaca, NY, USA, 1960.
15. Saparov, B.; Xia, S.-Q.; Bobev, S. Synthesis, structure and bonding of the Zintl phase $Ba_3Cd_2Sb_4$. *Inorg. Chem.* **2008**, *47*, 11237–11244. [[CrossRef](#)]
16. Saparov, B.; He, H.; Zhang, H.; Greene, R.; Bobev, S. Synthesis, crystallographic and theoretical studies of the new Zintl phases $Ba_2Cd_2Pn_3$ ($Pn = As, Sb$), and the solid solutions $(Ba_{1-x}Sr_x)_2Cd_2Sb_3$ and $Ba_2Cd_2(Sb_{1-x}As_x)_3$. *Dalton Trans.* **2010**, *39*, 1063–1070. [[CrossRef](#)]
17. Saparov, B.; Bobev, S. Isolated $[ZnPn_2]^{4-}$ chains in the Zintl phases Ba_2ZnPn_2 ($Pn = As, Sb, Bi$)—Synthesis, structure and bonding. *Inorg. Chem.* **2010**, *49*, 5173–5179. [[CrossRef](#)]
18. Nesper, R. The Zintl-Klemm concept—A historical survey. *Z. Anorg. Allg. Chem.* **2014**, *640*, 2639–2648. [[CrossRef](#)]
19. Nuspl, G.; Polborn, K.; Evers, J.; Landrum, G.A.; Hoffmann, R. The four-connected net in the $CeCu_2$ structure and its ternary derivatives. Its electronic and structural properties. *Inorg. Chem.* **1996**, *35*, 6922–6932. [[CrossRef](#)]
20. Savelsberg, G.; Schäfer, H. Ternaere Pnictide und Chalkogenide von Alkalimetallen und IB-bzw. IIB-Elementen. *Z. Naturforsch.* **1978**, *33B*, 370–373. [[CrossRef](#)]
21. Bobev, S.; Sevov, S.C. Five ternary Zintl phases in the systems alkali metal–indium–bismuth. *J. Solid State Chem.* **2002**, *163*, 436–448. [[CrossRef](#)]
22. SMART, Version 2.10; Bruker Analytical X-ray Systems, Inc.: Madison, WI, USA, 2003.
23. SAINT, Version 6.45; Bruker Analytical X-ray Systems, Inc.: Madison, WI, USA, 2003.
24. SADABS, Version 2.10; Bruker Analytical X-ray Systems, Inc.: Madison, WI, USA, 2003.
25. Sheldrick, G.M. Crystal structure refinement with SHELXL. *Acta Crystallogr. Sect. C* **2015**, *71*, 3–8. [[CrossRef](#)] [[PubMed](#)]